

Control of daughter centriole formation by the pericentriolar material

Control of centriole duplication

**Jadranka Loncarek¹, Polla Hergert¹, Valentin Magidson¹,
and Alexey Khodjakov^{1,2,*}**

¹Division of Molecular Medicine, Wadsworth Center, Albany, New York State Department of Health, Albany, New York 12201-0509

²Marine Biological Laboratory, Woods Hole, Massachusetts 02543

*Correspondence should be addressed to AK (Wadsworth Center, PO Box 509, Albany, NY 12201-0509, phone: (518)486-5339; fax: (518)486-4901; E-mail: khodj@wadsworth.org)

Abbreviations: PCM, pericentriolar material; HU, hydroxyurea; LUT, look-up table.

Controlling the number of its centrioles is vital for the cell as supernumerary centrioles result in multipolar mitosis and genomic instability^{1,2}. Normally, just one daughter centriole forms on each mature (mother) centriole^{3,4}; however, a mother centriole can produce multiple daughters within a single cell cycle^{5,6}. The mechanisms that prevent centriole ‘overduplication’ are poorly understood. Here we use laser microsurgery to test the hypothesis that attachment of the daughter centriole to the wall of the mother inhibits formation of additional daughters^{7,8}. We show that physical removal of the daughter induces reduplication of the mother in S-arrested cells. Under conditions when multiple daughters simultaneously form on a single mother, all of these daughters must be removed to induce reduplication. Intriguingly, the number of daughter centrioles that form during reduplication does not always match the number of ablated daughter centrioles. We also find that exaggeration of the pericentriolar material (PCM) via overexpression of the PCM protein pericentrin⁹ in S-arrested CHO cells induces formation of numerous daughter centrioles. We propose that the size of the PCM cloud associated with the mother centriole restricts the number of daughters that can form simultaneously.

A typical centrosome in an animal cell consists of two microtubule-based cylindrical structures, termed the centrioles, surrounded by a cloud of pericentriolar material (PCM). Most of the components responsible for the major centrosomal functions, for example, the γ -tubulin ring complex, reside in the PCM. However, in the absence of centrioles, the PCM cloud becomes structurally unstable, and eventually disperses¹⁰. Thus, the number of centrioles ultimately defines the number of centrosomes in the cell.

Normally, in somatic cells new ('daughter') centrioles form in association with mature ('mother') centrioles. This process, known as “centriole duplication”, is initiated when cells

enter S phase, and the daughter centriole remains associated with its mother, in a strictly orthogonal configuration (i.e., ‘diplosome’), until the second half of the ensuing mitosis¹¹⁻¹³. Recent work suggested that as long as the daughter remains attached to the mother formation of additional daughters is not possible^{7,8}.

A key question is how the cell ensures that a mother centriole produces one and only one daughter, in a given cell cycle. It has been postulated that the mother centriole contains a site (‘template’) on which formation of the daughter centriole is initiated when cytoplasmic conditions become favorable¹⁴. Alternatively, centrioles have been viewed as a ‘solid state assembly platform’ that impose steric constraints thus regulating the number of daughter centrioles that can assemble in their vicinity⁶. Multiple daughters can form simultaneously on the same mother upon overexpression of certain centriolar proteins^{4,15,16}.

We sought to determine whether physical ablation of one centriole within the diplosome with a laser beam would induce reduplication of the remaining centriole in HeLa cells. We used a centrin-GFP fusion protein¹⁷ as a reliable centriolar marker that allowed us to detect the earliest stages of centriole duplication in live cells (Supplementary Text I, Figs. S1, S2). Further, HeLa cells possess a stringent mechanism by which centriole reduplication during S-arrest is prevented (Supplementary Text II, Fig. S3).

Upon ablation of the daughter centriole within a diplosome, the remaining mother consistently (20 of 20 experiments) developed a new daughter (Figs. 1A, S4). The interval between the ablation of the original daughter and formation of the new one was variable (1-6 hrs [see Methods], average = 2.8 ± 1.5 hr, Fig. 1). Same-cell LM-EM analyses revealed that new daughters were morphologically normal. When cells were fixed for EM at the early stages of centriole reduplication, the younger daughter centriole formed on the reduplicating mother was significantly smaller than the older daughter in the non-irradiated diplosome (Fig. 1B; N=3). At later stages, the sizes of the younger and older daughters became more

similar (N=3; data not shown). It is noteworthy that even in control diplosomes, daughter centrioles were consistently shorter than their mothers (<300 nm vs. ~450 nm) in all examined cells fixed 10-40 hr after addition of hydroxyurea (HU) (see Fig. S1).

We also succeeded to repeatedly ablate daughter centrioles reforming on the same mother twice (Fig. 1C; N=2), and even three times (not shown, N=1). Thus, a single mother centriole is capable of repeatedly duplicating at least four times in the same cell cycle. However, continuous association of the daughter centriole with its mother prevents the mother centriole from reduplicating.

When only the mother centriole was ablated, within a diplosome, the remaining daughter did not duplicate in HeLa cells (N=16). In six of these cells the centrin-GFP signal gradually degraded as to become undetectable 24 hr after ablation. Furthermore, serial-section EM analysis of one cell that still contained a centrin spot 26 hr after ablation (Fig. 1D) revealed that this spot did not correspond to a morphologically recognizable centriole (not shown). Immunofluorescence staining for γ -tubulin demonstrated that daughter centrioles fixed ~1 hr after ablation of the mother did not contain PCM (3 of 4, data not shown). Together, these results suggest that immature daughter centrioles precipitately released from their mother in S-phase arrested HeLa cells cannot maintain their association with the PCM, and ultimately deteriorate.

Several cell lines, including Chinese Hamster Ovary (CHO) cells, have been shown to escape the reduplication block and to amplify centrioles, when arrested in S phase⁵. In these cells, centrioles undergo repetitive cycles of duplication and disengagement (Supplementary Text II, Fig. S3B). Intriguingly, in ~10% of S-phase arrested CHO cells, reduplicating mother centrioles develop two daughters, thereby forming “triplosomes” (Fig. 2). Triplosomes exhibit several characteristic features that enabled them to be discriminated from random agglomerations of adjacent but independent centrioles. In live cells, the

movements of centrioles within triplosomes were coordinated, revealing that the centrioles were interconnected (Video S6). In contrast, movements of adjacent but independent centrioles were not coordinated (Video S7). Serial-section EM revealed that centrioles in triplosomes were oriented in a flower-petal configuration (Fig. 2), although the angle between the daughter centrioles varied. Occasionally, more than two daughters centrioles assembled in association with a single mother (Fig. S5).

We thought to determine if removal of a single daughter from the triplosome will result in the formation of a new daughter, or if both daughters must be removed to trigger mother centriole reduplication. First we confirmed that like in HeLa cells ablation of the single daughter centriole within a diplosome in a CHO cell induced reduplication of the remaining mother centriole (Fig. 3A; 20 of 20 cells). Interestingly, in two of these cells, mother centrioles formed two daughter centrioles each during reduplication (Fig. 3B). This phenomenon and its frequency was consistent with the observation of the triplosome formation during reduplication of mother centrioles in non-irradiated CHO cells. In contrast to HeLa cells, daughter centrioles were also able to replicate after ablation of the mother (Fig.3C).

Ablation of both daughters in the triplosome induced reduplication of the mother (N=4). However, in all four cases only a single daughter centriole developed during reduplication (Fig. 3D). In contrast, when just one of the two daughter centrioles in a triplosome was ablated, the ablated daughter did not regenerate for as long as the mother and second daughter remained engaged (Fig. 3E; N=6). Then, upon natural disengagement, which occurred 15-25 hr after the operation, the mother centriole reduplicated in at least two of the six cells. Surprisingly, if just the mother centriole was ablated in a triplosome, the two daughters continued to move in a coordinated fashion (Fig. S6, Video S8; N=8). Due to the large number of centrioles present in CHO cells after 48-72

hr in HU, it was not possible for us to unequivocally determine if these pairs of daughter centrioles ultimately disengaged and duplicated.

Thus, when multiple daughters are associated with a single mother all of these daughters must be removed to trigger mother centriole reduplication. Intriguingly, the number of daughter centrioles formed during reduplication does not necessarily match the number of the original daughter centrioles. This raises a question of what defines the number of daughter centrioles.

In addition to canonical duplication, centrioles can arise de novo in a range of cell types¹⁸⁻²⁰. In this pathway, centrioles form inside a cloud of PCM-like material that contains typical centrosomal proteins such as γ -tubulin and pericentrin^{18,21}. This suggests that PCM clouds can provide localized environment that supports centriolar assembly. If true, the size of the PCM cloud associated with the mother centriole could limit the number of forming daughters, and exaggeration of the PCM should allow simultaneous formation of numerous daughters. We tested this prediction by overexpressing pericentrin, a major component of the PCM⁹. Importantly, centrioles can duplicate in cells depleted of pericentrin⁶, suggesting that in contrast to other PCM components²² pericentrin is not directly involved in centriole assembly.

We found that overexpression of HA-tagged mouse pericentrin at high level in S-phase arrested CHO cells induced formation of large PCM clouds that also contained variable numbers of centrin-GFP aggregates embedded into a more diffuse centrin-GFP cloud (Fig.4). Two of the centrin-GFP aggregates were always significantly brighter than the rest (Fig.4C). Same-cell correlative LM/EM analyses revealed that these two aggregates corresponded to mother centrioles. Many, although not all, of the dimmer aggregates represented centrioles at different levels of maturation. Often these centrioles were short (Fig. S7A), although some could reach a length typical for a mature centriole (Fig. S7B).

These short centrioles were not paired in the typical diplosome structures but oriented randomly within the cloud of PCM. The total number of centrioles in pericentrin-overexpressing cells exceeded the number of centrioles that would be expected to arise via repetitive rounds of centriole reduplication (Fig. S4).

Several studies reveal that centriole assembly is driven by the activity of Plk-4 kinase and requires SAS-6, a protein that remains associated with the proximal end of the forming centriole⁶. In the typical diplosome SAS-6 localizes near the wall of the mother centriole at its proximal end. However, we find that in triplosomes localization of SAS-6 spots is more variable. While SAS-6 spots always reside within the PCM, often they are not in the immediate vicinity of the mother centriole (Fig. 4D). The separation between the SAS-6 spots and mother centrioles is even more prominent within large centrosomes that form upon pericentrin overexpression (Fig. 4D).

Several structural data suggest that daughter centrioles are not attached to the wall of their mother at the early stages of their formation. For example, procentrioles have been shown to be less stringently oriented with respect to their mothers than older (>150-nm) daughters (Fig. S2, ref.^{11,23}). Further, even for relatively large daughter centrioles, their radial orientation with respect microtubule triplets in the mother is not fixed (Fig. S8A). Another observation that suggest that centriole formation is not initiated at a particular fixed spot on the mother centriole is evident in some of our ablation operations when the laser beam inadvertently damaged the wall of the mother centriole at the site of the original daughter. The new daughter formed at a different site, sometimes as distantly as on the opposite side of the mother (Fig. S8B).

Together, these data suggest that formation of daughter centrioles is initiated within the PCM cloud but not necessarily at the wall of the mother centriole. We propose that the role of the mother is not to provide a template for the assembly of daughter centrioles but to organize and maintain a single compact cloud of PCM, thereby restricting the size of the

environment where centrioles assembly is promoted. In our view, centriole duplication and the de novo assembly pathway are based on the same mechanism. Indeed, recent data have revealed that the de novo assembly requires the same molecular machinery as does centriole duplication^{24,25}. Our hypothesis can also explain why the de novo pathway is efficiently inhibited in the presence of mature centrioles^{19,26}: while small aggregates of PCM continuously form in the cytoplasm of centriolar cells, these aggregates are effectively transported to and incorporated into the existing centrosome²⁷ before they reach the size sufficient to initiate centriole assembly. In the absence of resident centrioles, the randomness of the aggregation of PCM within the cytoplasm has the effect that the number of centrioles becomes unpredictable and their formation requires longer time^{18,19}.

Acknowledgements

We thank the members of our lab for fruitful discussions. Special thanks to Drs. Brian M. Davis and Igor B. Roninson for their help with construction the centrin-GFP lentivirus and Dr. Yimin Dong for assistance with 3-D reconstructions. We also thank Drs. Kip Sluder, Conly Rieder, and Michael Koonce, for critical comments on the manuscript. This work was supported by grants from the National Institutes of Health (GM GM59363) and the Human Frontiers Science Program (RGP0064). Construction of our laser microsurgery workstation was supported in part by a fellowship from Nikon/Marine Biological Laboratory (A.K.). We acknowledge use of the Wadsworth Center's Electron Microscopy Core Facility.

Author contributions

Experiments were conducted by J.L.; P.H. was responsible for EM preparation and data collection; V.M. designed, assembled, and maintained the laser microsurgery workstation; A.K. directed the work. Experiments were planned by J.L. and A.K.

Competing financial interests

The authors declare that they have no competing financial interests.

Materials and Methods

Cell culture and drug treatments

The CHO K-1 cell line was obtained from the American Type Culture Collection (ATCC, Manassas, VA), and cells were cultured in F-12 medium (Gibco), supplemented with 10% fetal calf serum (Cellgro), 100 U of penicillin, and 1 µg/ml streptomycin (Gibco). A lentivirus expression system (LentiLox3.7 vector, <http://csbi.mit.edu/rnai/vector>) was used for stable expression of centrin-1-GFP in these cells. HeLa cells expressing centrin-1-GFP¹⁷ were cultured in DMEM (Gibco), supplemented with 10% serum, 100 U penicillin, and 1 µg/ml streptomycin. Both cell lines were maintained in a humidified incubator at 37°C in 5% CO₂ atmosphere. Mitotic cells were collected by shake-off from untreated asynchronous populations and were then plated on glass cover slips in complete growth medium containing 2-mM hydroxyurea (Sigma). For microscopy, coverslips with cells were mounted on Rose chambers in CO₂-independent medium (Gibco) supplemented by 10% fetal calf serum, penicillin, streptomycin, and 2 mM HU. During long-duration experiments, Rose chambers were perfused once per day with fresh medium. Hydroxyurea was prepared by dilution of a 1M H₂O stock solution in culture media.

Laser microsurgery and fluorescence imaging

Laser microsurgery was conducted on a custom-assembled microscopy workstation centred on a Nikon TE2000-E2 microscope (Nikon Instruments, Melville, NY). The detailed layout of the system is presented elsewhere²⁸. In brief, 532-nm 8-ns laser pulses were generated by a Q-switched Nd:YAG laser (Diva II; Thales Lasers, Paris, France) run at 20-Hz repetition rate. The collimated laser beam was expanded to ~8 mm to fill the aperture of a 100X 1.4 NA PlanApo lens and was delivered through a dedicated epi-port. About 3-5

laser pulses (up to 0.5 sec) are required to destroy a centriole. After laser ablation of the centriole(s), the position of the experimental cell was marked with a diamond scribe and the cell was filmed as described previously¹⁹, except that fluorescence images were recorded in confocal mode (spinning-disk Yokogawa GSU-10 unit) on a back-illuminated EM CCD camera (Cascade512B, Photometrics, Tucson, AZ). All fluorescence images are presented here as maximal intensity projections of 3-D data sets collected at 0.25- μ m Z steps. All light sources were shuttered by either fast mechanical shutters (Vincent Associates) or AOTF (Solamere Technology Group) so that cells were exposed to blue light only during image acquisition and/or laser operations. The system was driven by IPLab software (Scianalytics).

Because our ability to detect the initial stages of daughter centriole formation depended on the orientation of the diplosome (Fig. S4) we often collected several (3-7) Z-series of the same centrosome at each time point (Fig.S4).

Centrin-GFP at the centriole is in continuous dynamic exchange with the cytoplasmic pool so that photobleached centrioles recover ~50% of their original intensity in 60 min²⁸. Thus, a rapid reappearance of centrin-GFP signal at the location of irradiated centriole can formally be due to fluorescence recovery after photobleaching. For this reason, in our experiments we only followed those cells where re-appearance of centrin-GFP spot occurred in more than 1 hr. This ensures that in all cases presented in the manuscript centrioles were truly ablated. However, this also implies that we disregarded potential formation of daughter centrioles in less than 1 hr.

Electron microscopy

For comparative LM/EM analysis, the cells were fixed in PBS containing 2.5% glutaraldehyde, directly in Rose chambers. Fluorescence images of centrioles were taken immediately prior to and immediately after fixation. Embedding and serial sectioning were

performed according to established protocols¹⁹. 80-nm sections were examined in a Zeiss 910 microscope at 100 KV and were photographed on film. Film negatives were subsequently scanned and contrast-adjusted in Adobe PhotoShop CS (Adobe Systems, Palo Alto, CA).

Pericentrin overexpression

A HA-labeled full-length mouse pericentrin²⁹ was kindly provided by Dr. Stephen Doxsey (UMasss, Medical School). CHO cells synchronized and treated with 2-mM HU as described above were transfected 6 hr after mitotic shake off. Transfections (3 µg of DNA per 5-cm culture dish) were carried out with Lipofectamine Plus (Invitrogen) according to the manufacturers instructions.

Immunostaining

Cells were fixed in 2% formaldehyde for 10 min at room temperature and post-fixed with cold methanol for 2 min (for double γ-tubulin/HA staining) or in cold methanol for 7 minutes (for double Sas6/γ-tubulin staining). γ-tubulin was visualized by rabbit (C-20, Santa Cruz) or by mouse (GTU-88, SIGMA) antibodies. Anti HA antibodies (HA12CA5) were used for detection of pericentrin-HA fusion protein. Anti-SAS6 antibody³⁰ was kindly provided by Dr. Pierre Gonczy (ISREC, Switzerland).

3-D datasets of fixed cells were collected on a DeltaVision workstation and were deconvolved using SoftWorX 2.1 software (Applied Precision). Surface-rendered models of centrosomes presented in Videos S9-S12 were computed using Amira 3.1 software (Mercury Computer Systems). Isosurface of γ-tubulin distribution represents 25% of the maximal intensity.

References

1. Nigg,E.A. Centrosome aberrations: cause or consequence of cancer progression? *Nature Reviews Cancer* **2**, 815-825 (2002).
2. Sluder,G. & Nordberg,J.J. The good, the bad and the ugly: the practical consequences of centrosome amplification. *Curr. Opinion in Cell Biol.* **16**, 49-54 (2004).
3. Tsou,M.-F.T. & Stearns,T. Controlling centrosome number: licenses and blocks. *Curr. Opinion in Cell Biol.* **18**, 74-78 (2006).
4. Duensing,A. et al. Centriole overduplication through the concurrent formation of multiple daughter centrioles at single maternal templates. *Oncogene* **26**, 6280-6288 (2007).
5. Balczon,R. et al. Dissociation of centrosome replication events from cycles of DNA synthesis and mitotic division in hydroxyurea-arrested Chinese hamster ovary cells. *J. Cell Biol.* **130**, 105-115 (1995).
6. Kleylein-Sohn,J. et al. Plk4-induced centriole biogenesis in human cells. *Developmental Cell* **13**, 190-202 (2007).
7. Wong,C. & Stearns,T. Centrosome number is controlled by a centrosome-intrinsic block to reduplication. *Nature Cell Biology* **5**, 539-544 (2003).
8. Tsou,M.F. & Stearns,T. Mechanism limiting centrosome duplication to once per cell cycle. *Nature* **442**, 947-951 (2006).
9. Dictenberg,J.B. et al. Pericentrin and gamma-tubulin form a protein complex and are organized into a novel lattice at the centrosome. *J. Cell Biol.* **141**, 163-174 (1998).
10. Bobinnec,Y. et al. Centriole disassembly in vivo and its effect on centrosome structure and function in vertebrate cells. *J. Cell Biol.* **143**, 1575-1589 (1998).
11. Kuriyama,R. & Borisy,G.G. Centriole cycle in Chinese hamster ovary cells as determined by whole-mount electron microscopy. *J. Cell Biol.* **91**, t-21 (1981).
12. Vorobjev,I.A. & Chentsov,Y.S. Centrioles in the cell cycle. I. Epithelial cells. *J. Cell Biol.* **93**, 938-949 (1982).
13. Paintrand,M., Moudjou,M., Delacroix,H., & Bornens,M. Centrosome organization and centriole architecture: their sensitivity to divalent cations. *J. Struct. Biol.* **108**, 107-128 (1992).
14. Marshall,W.F. What is the function of centrioles? *Journal of Cellular Biochemistry* **100**, 916-922 (2007).
15. Vidwans,S.J., Wong,M.L., & O'Farrell,P.H. Anomalous centriole configurations are detected in Drosophila wing disc cells upon Cdk1 inactivation. *J. Cell Sci.* **116**, 137-143 (2003).

16. Habedank,R., Stierhof,Y.D., Wilkinson,C.J., & Nigg,E.A. The Polo kinase Plk4 functions in centriole duplication. *Nature Cell Biology* **7**, 1140-1146 (2005).
17. Piel,M., Meyer,P., Khodjakov,A., Rieder,C.L., & Bornens,M. The respective contributions of the mother and daughter centrioles to centrosome activity and behavior in vertebrate cells. *J. Cell Biol.* **149**, 317-330 (2000).
18. Khodjakov,A. *et al.* De novo formation of centrosomes in vertebrate cells arrested during S phase. *J. Cell Biol.* **158**, 1171-1181 (2002).
19. La Terra,S. *et al.* The de novo centriole assembly pathway in HeLa cells: cell cycle progression and centriole assembly/maturation. *J. Cell Biol.* **168**, 713-720 (2005).
20. Uetake,Y. *et al.* Cell cycle progression and de novo centriole assembly after centrosomal removal in untransformed human cells. *J. Cell Biol.* **176**, 173-182 (2007).
21. Kim,H.-K. *et al.* De novo formation of basal bodies in *Naegleria gruberi* : regulation by phosphorylation. *J. Cell Biol.* **169**, 719-724 (2005).
22. Dammermann,A. *et al.* Centriole assembly requires both centriolar and pericentriolar material proteins. *Developmental Cell* **7**, 815-829 (2004).
23. Pelletier,L., Toole,E., Schwager,A., Hyman,A.A., & Muller-Reichert,T. Centriole assembly in *Caenorhabditis elegans*. *Nature* **444**, 619-623 (2006).
24. Rodrigues-Martins,A., Riparbelli,M., Callaini,G., Glover,D.M., & Bettencourt-Dias,M. Revisiting the role of the mother centriole in centriole biogenesis. *Science* **316**, 1046-1050 (2007).
25. Peel,N., Stevens,N.R., Basto,R., & Raff,J.W. Overexpressing centriole-replication proteins in vivo induces centriole overduplication and de novo formation. *Curr. Biol.* **17**, 834-843 (2007).
26. Marshall,W.F., Vucica,Y., & Rosenbaum,J.L. Kinetics and regulations of de novo centriole assembly: implications for the mechanism of centriole duplication. *Curr. Biol.* **11**, 308-317 (2001).
27. Young,A., Dictenberg,J.B., Purohit,A., Tuft,R., & Doxsey,S.J. Cytoplasmic dynein-mediated assembly of pericentrin and γ -tubulin onto centrosomes. *Molec. Biol. of the Cell* **11**, 2047-2056 (2000).
28. Magidson,V., Loncarek,J., Hergert,P., Rieder,C.L., & Khodjakov,A. Laser microsurgery in the GFP era: A cell biologist's perspective in *Laser Manipulations of Cells and Tissues* (eds. Berns,M.W. & Greulich,K.O.) 237-266 (Elsevier, 2007).
29. Purohit,A., Tynan,S.H., Vallee,R.B., & Doxsey,S.J. Direct interaction of pericentrin with cytoplasmic dynein light intermediate chain contributes to mitotic spindle organization. *J. Cell Biol.* **147**, 481-492 (1999).
30. Strnad,P. *et al.* Regulated HsSAS-6 levels ensure formation of a single procentriole per centriole during the centrosome duplication cycle. *Developmental Cell* **13**, 203-213 (2007).

Figures

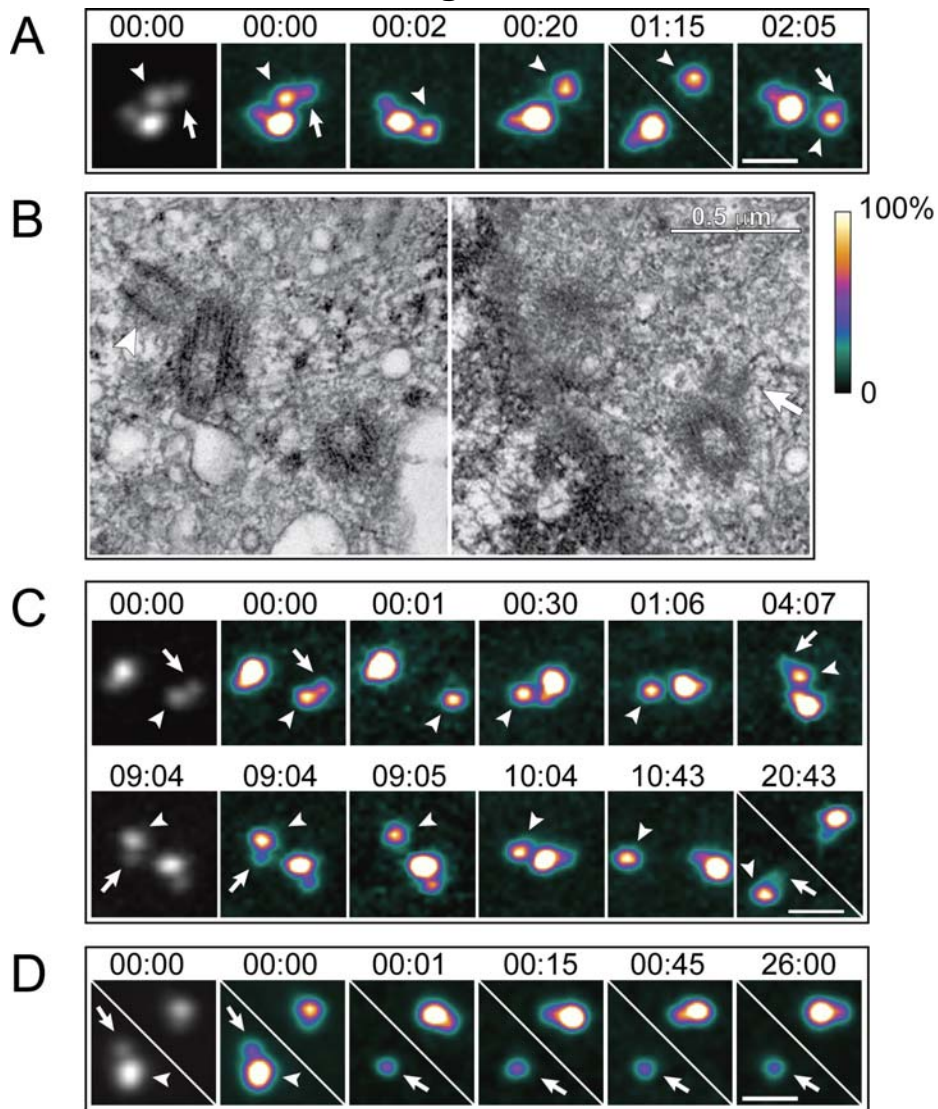


Figure 1. Laser ablation of daughter centrioles induces reduplication of the remaining mothers in S-phase arrested HeLa cells. **(A)** Daughter centriole in one of the two diplosomes was ablated (arrow in 00:00). The mother remained single for >1 hr , and then developed a “shadow” (arrow in 02:07, also see Fig.S4), indicating formation of a new daughter. This cell was fixed for EM at 02:08. **(B)** Selected 80-nm EM sections from the complete series of the cell presented in (A). Notice that the new daughter centriole (arrow) is significantly smaller than the daughter in the other, non-irradiated diplosome (arrowhead). **(C)** Repetitive ablations of daughter centrioles. After ablation of the first daughter (arrow in 00:00), the mother (arrowheads) developed a new daughter in ~4 hr (arrow in 04:07). This daughter was subsequently ablated (arrow in 09:04) and ~10 hr later another daughter developed (arrow in 20:43). Notice that the centrioles in the non-irradiated diplosome remained engaged throughout the experiment. EM analysis confirmed that the shadow seen in 20:43 was in fact a daughter centriole. **(D)** Mother centriole in one of the two diplosomes was ablated (arrowhead in 00:00) and the remaining daughter (arrows) did not duplicate. All images in A, C, and D are maximal intensity projections of complete Z-series through the centrosome. Due to the significant differences in fluorescence intensity between the mature and newly formed centrioles, it is impossible to reproduce the two types simultaneously through use of a linear grey-scale look-up table (LUT). Instead, a pseudo-colour intensity LUT (shown to the right of panel B) has been applied to the images. The first image in each series is also presented in contrast-enhanced grey-scale (non-linear γ factor). Scale bars in A, C, and D represent 1 μm. Time stamps in panels A, C, and D are in hours : minutes.

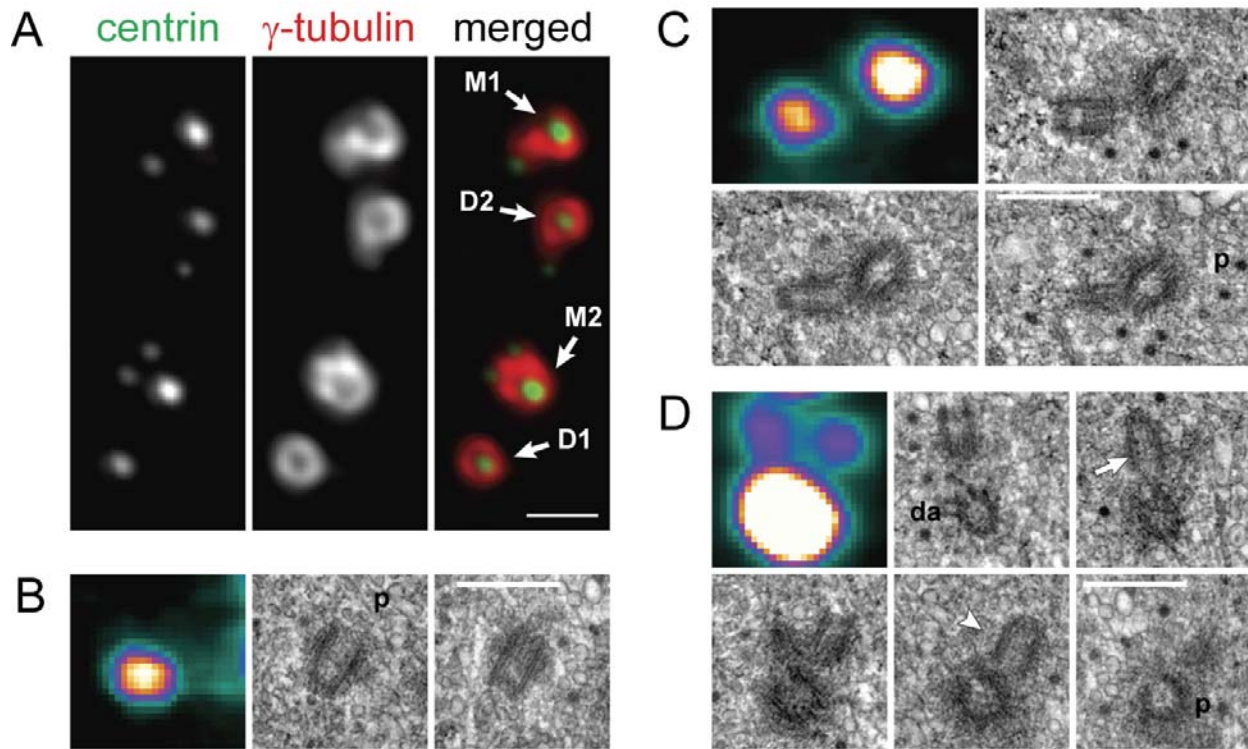


Figure 2. Examples of centriolar configurations in S-phase arrested CHO cells. **(A)** Centrosomes in a typical CHO cell after 38 hr in 2-mM hydroxyurea (also see Fig. S4), as visualized by immunostaining. This centrosome contained two brighter mother centrioles (M1 and M2) and two dimmer daughter centrioles formed in the first round duplication (D1 and D2). At the time of fixation, both mothers were reduplicating. Centrioles M1 and D2 were associated with single daughters thus forming classical diplosomes, while centriole M2 was associated with two daughters, thus forming a triplosome. The other daughter centriole (D1) remained single during the second round of replication. Scale bar = 1 μ m. **(B – D)** Centriole ultrastructure in a typical cell fixed after 37 hr in HU. (B) single centriole, (C) diplosome, and (D) triplosome. The first image in each panel presents a maximal-intensity projections of the centrin-GFP fluorescence recorded immediately after fixation. These images are pseudocolored with the same LUT as in Fig.1. The remaining images in each panel depict selected consecutive 80-nm EM sections from the complete series through the cell. Proximal ends of mother centrioles are marked 'p'. In contrast to the behaviour observed in HeLa cells (Figs. 1B, S1), daughter centrioles in S-phase arrested CHO cells develop to full length (~400 nm). Notice that daughter centrioles are orthogonal to their mothers in both the diplosome (C) and triplosome (D). One daughter in the triplosome (arrow in D) is closer to the proximal end of the mother than is the other daughter (arrowhead in D). Also note that the triplosome in this cell was formed by the oldest mother centriole, which contained the greatest amount of centrin-GFP, and was the only centriole in the cell to carry distal appendages (marked 'da'). Scale bars in C-E = 0.5 μ m.

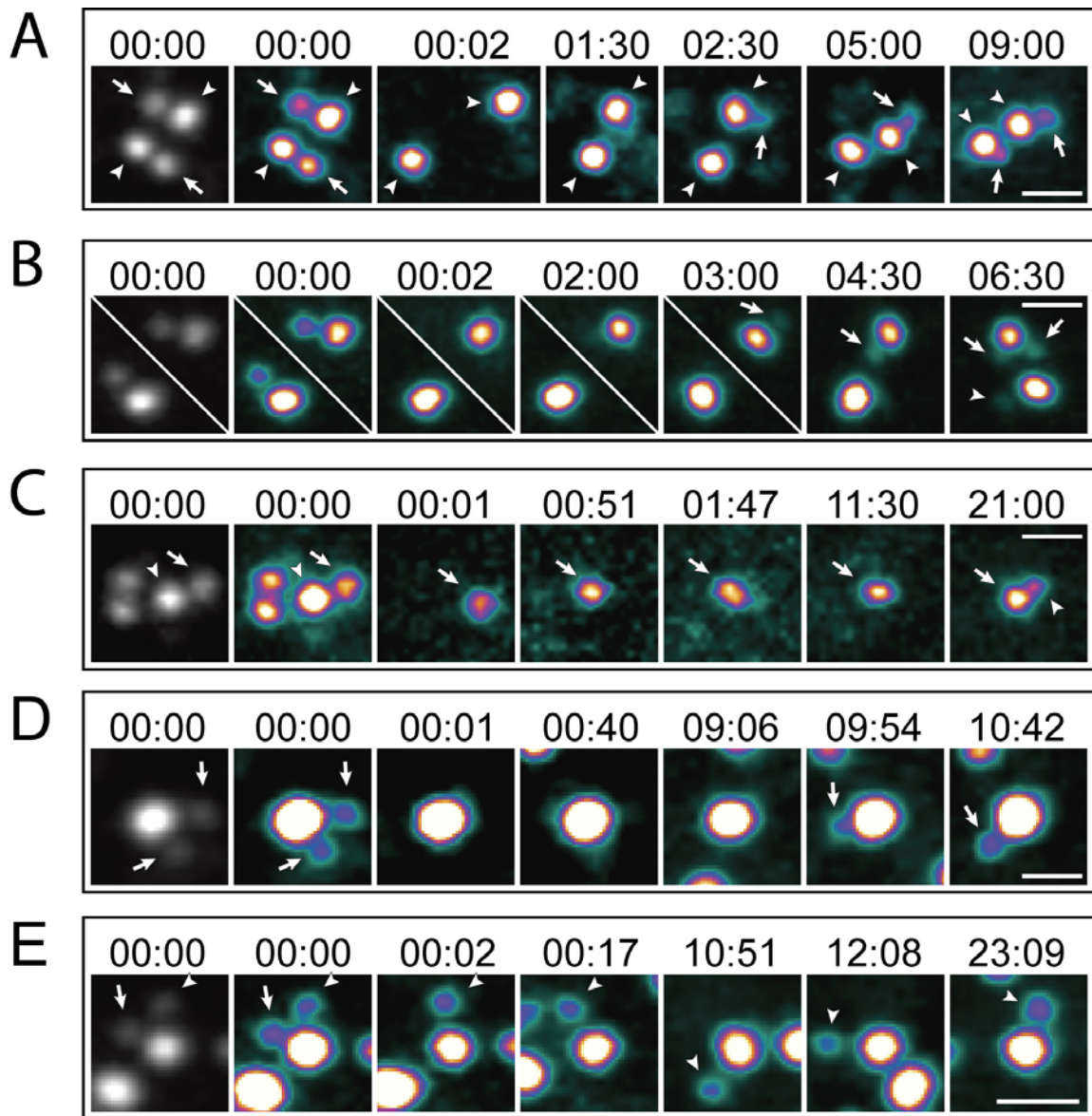


Figure 3. Ablation of all daughter centrioles within a centrosome induces reduplication of the mother in S-phase arrested CHO cells. **(A)** In this cell, daughter centrioles in both diplosomes were ablated (arrows in 00:00). Both mother centrioles (arrowheads) remained single for more than 1 hr. Then, one of the mothers developed a new daughter (arrow in 02:30), while the second mother remained single. Approximately 9 hr after ablation, the second mother also developed a new daughter centriole (arrow in 09:00). **(B)** An example of triplosome formation after ablation of the original daughter centriole. Both daughter centrioles were ablated, as in (A). However, one of the mothers in this cell developed two daughter centrioles (arrows in 03:00, 04:30, and 06:30). Formation of the two daughters was not simultaneous. However, at later time points the two daughters appeared to be of the same size (not shown). The second mother developed a single daughter centriole (arrowhead in 06:30). **(C)** In this cell the mother centriole in one of the diplosomes was ablated (arrowhead). Because the daughter and mother centrioles can undergo natural disengagement during the course of >20-hr long experiments, which complicates the analysis, the second diplosome was also completely ablated. As the result, the cell was left with just one daughter centriole (arrows). This centriole remained single for more than 11 hr but ultimately developed a daughter (arrowhead in 21:00). **(D)** Both daughters within a triplosome (arrows in 00:00) were ablated. The mother remained a single centriole for ~9 hrs and then developed a new daughter (arrows in 09:54 and 10:42). **(E)** Just one of the two daughters in a triplosome was ablated (arrows in 00:00) converting this triplosome into a diplosome. The other daughter centriole (arrowhead) remained engaged with the mother for more than 24 hrs, and the ablated daughter did not regenerate. Time stamps in hours : minutes. Scale bars = 1 μ m. Same LUT as in Fig.1.

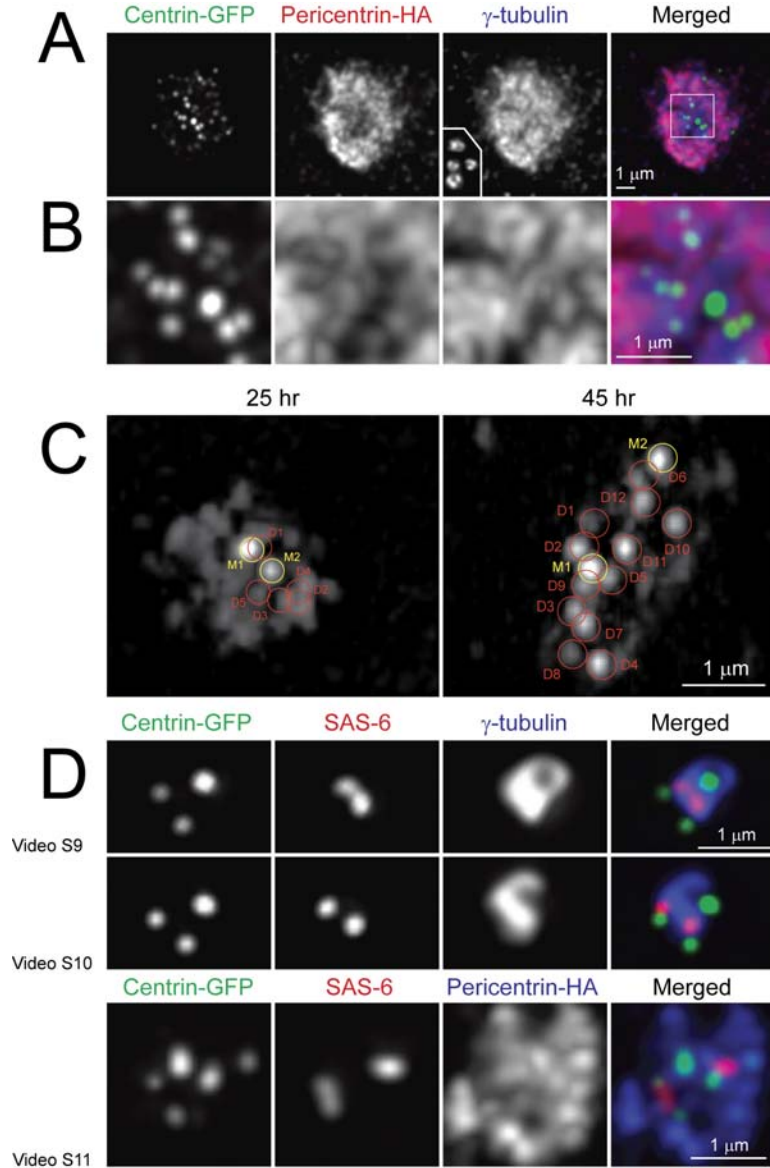


Figure 4. Effects of PCM exaggeration on the number of daughter centrioles. **(A)** Overexpression of pericentrin in S-phase arrested CHO cells results in the formation of a large cloud of pericentriolar material that contains numerous centrin-GFP aggregates cloud overexpressing pericentrin. (A) Lower-magnification view of the centrosome in a cell expressing pericentrin (visualized with an anti-HA antibody). Inset in the γ -tubulin frame depicts the size of the γ -tubulin cloud of normal centrosomes in CHO cells shown at the same magnification. (B) Higher-magnification view of the region boxed in “(A) Merged”. **(C)** Some but not all centrin aggregates in pericentrin-overexpressing cells are centrioles. Centrin-GFP distribution in two cells that were analyzed by serial-section EM (see Fig. S7 for EM data). In the cell fixed 25 hr after transfection (left frame) centrin-GFP distribution is generally diffused with two brighter and several dimmer discrete spots. The brighter spots (M1 and M2) correspond to full-length mother centrioles while five of the dimmer spots (D1-D5) correspond to short randomly-oriented daughter centrioles (see Fig. S7A). In the cell fixed 45 hrs after transfection (right frame) discrete centrin spots are more prominent. Two brightest spots (M1 and M2) correspond to mother centrioles and twelve of the dimmer spots (D1-D12) correspond to daughter centrioles (see Fig. S7B). **(D)** 3-D organization of centrosomes with multiple daughter centrioles. Notice that centrin spots corresponding to the distal ends of centrioles may reside within the γ -tubulin cloud or protrude outside. In contrast, the proximal ends of daughter centrioles (marked by SAS-6) consistently reside within the PCM although they are not always in the proximity of the mother centriole . See Videos 9-11 for surface-rendered models of the centrosomes presented here.